



Dynamic behavior of cracked simply supported pipe conveying fluid with moving mass

Han-Ik Yoon^{a,*}, In-Soo Son^b

^a*Department of Mechanical Engineering, Dong-eui University, San 24, Gaya3-dong Busanjin-gu, Busan 614-714, Korea*

^b*Department of Mechanical Engineering, Graduate School of Dong-eui University, Busan 614-714, Korea*

Received 5 October 2004; received in revised form 20 July 2005; accepted 17 September 2005

Available online 20 December 2005

Abstract

In this paper we studied about the effect of the open crack and a moving mass on the dynamic behavior of a simply supported pipe conveying fluid. The equation of motion is derived by using Lagrange's equation and analyzed by numerical method. The crack section is represented by a local flexibility matrix connecting two undamaged pipe segments. That is, the crack is modeled as a rotational spring. This matrix defines the relationship between the displacements and forces across the crack section and is derived by applying fundamental fracture mechanics theory. The influences of the crack severity ratio, the position ratio of the crack, the moving mass and its velocity, the velocity of fluid, and the coupling of these factors on the vibration mode, the frequency ratio, and the mid-span displacement of the simply supported pipe are depicted.

© 2005 Published by Elsevier Ltd.

1. Introduction

The detection and control of damage in mechanical structures are important concerns of engineering communities. When a structure is subjected to damage its dynamic response is varied due to the change of its mechanical characteristics. In this framework the interesting issue is the effect of an open crack on the structural response. And the effect of moving mass on the structures and the machines is an important problem both in the field of transportation and on the design of machining processes. And the fluid flowing inside the pipe acts as the concentrated tangential follower force at the tip of the pipe, and exerts a lot of influences on the dynamic characteristic of a pipe. Therefore, a large number of papers have presented about the dynamic behavior of fluid-conveying pipes since the early 1960s. The transfer of energy between the flowing fluid and the pipe was discussed by Benjamin [1]. The problem of flutter induced by a pure rocket thrust, which has applications to missiles, spacecraft and space structure, is also closely related [2]. Lee [3] studied the dynamic response of a clamped–clamped beam acted upon by a moving mass. He analyzed the problem of the moving mass separating from the beam by monitoring the contact forces between them. A lot of studies about the dynamic behavior of a beam structure under moving load and moving mass were reported

*Corresponding author.

E-mail address: hiyoon@deu.ac.kr (H.-I. Yoon).

Nomenclature			
		q_n	deflection of pipe
		t_p	thickness of pipe
a_c	depth of crack	T_f	kinetic energy of fluid in pipe
A	cross-sectional area of pipe	T_m	kinetic energy of moving mass
b	half-length of crack	T_p	kinetic energy of pipe
C	flexibility matrix	u	velocity of fluid
d_n	deflection of pipe, dimensionless	U	velocity of fluid, dimensionless
E	Young's modulus	v	velocity of moving mass
I	second moment of area of the pipe cross-section	V_p	potential energy of pipe
J	strain energy density function	W_c	work done by conservative part of applied forces by fluid velocity
k	number of segment due to crack	W_{nc}	work done by non-conservative part of applied forces by fluid velocity
K_I	stress intensity factor (fracture mode I)	x_c	crack location
K_R	rotating spring coefficient	ν_p	Poisson's ratio
L	length of pipe	θ	half-angle of crack
L_a	Lagrangian	θ^*	half-angle of crack, dimensionless
m	mass per unit length of pipe	κ	shearing coefficient of cross-section of pipe
m_f	fluid mass per unit length of pipe	ξ	distance measured along pipe, dimensionless
m_m	moving mass	ξ_c	crack location, dimensionless
M_f	fluid mass per unit length of pipe, dimensionless		
M_m	moving mass, dimensionless		
n	number of generalized coordinates		

[4–6]. Recently, Mahmoud and Abou Zaid [7] used an equivalent static load approach to determine the stress intensity factors for a single- or double-edge crack in a beam subjected to a moving load. Chondros and Dimarogonas [8–10] studied the effect of the crack depth on the dynamic behavior of a cantilevered beam. They showed that the increase of the crack depth reduces the natural frequency of the beam. Also, they used energy method and a continuous cracked beam theory for analyzing the transverse vibration of cracked beams. Ostachowicz and Krawczuk [11] investigated the influence of the position and the depth of two open cracks upon the fundamental frequency of the natural flexural vibrations of a cantilever beam. To model the effect of the local stress in the crack, they introduced two different functions according to the symmetry of the crack. The dynamic characteristics of a cracked rotor supported on AMBs are studied; the effect of using optimal controller parameters on the dynamics of the active cracked rotor and the effects of crack on the control system are analyzed [12]. An equation of bending motion for Euler–Bernoulli beam containing pairs of symmetrical open cracks was derived by Christides and Barr [13]. The cracks were considered to be normal to the beam's neutral axis and symmetrical about the plane of bending. Dado and Abuzeid [14] studied the modeling and analysis algorithm for cracked Euler–Bernoulli beams by considering the coupling between the bending and axial modes of vibration. This algorithm is applied to the analysis of the vibration behavior of the cracked beam and particularly the natural frequency and mode shapes under the effect of added mass and rotary inertia at the free end. Liu et al. [15] examined the suitability of using coupled responses to detect damage in thin-walled tubular structures. By coupled response they referred to the ability of a structural member with a circumferential crack to experience composite vibration modes (axial and bending) when excited purely laterally. Zheng and Fan [16,17] studied the stability of a cracked Timoshenko beam column by modified Fourier series. Also, they present simple tools for the vibration and stability analysis of cracked hollow-sectional beams. Maiti et al. [18] have shown the results of study on crack detection in pipes filled with fluid by the theory analysis and the experiment. Recently, reviews on vibration of cracked structures were reported by Wauer [19] and Dimarogonas [20], and many studies investigated the dynamic response of a beam structure with a crack [21–30].

In this study, the crack effects on the dynamic behavior of the cracked pipe conveying fluid with the moving mass are investigated. That is, the influences of a crack, position of a crack and the velocity of the moving mass have been studied on the dynamic behavior of a simply supported pipe conveying fluid system. In addition, the influences of a fluid flow have studied on the dynamic characteristics of a cracked simply supported pipe with the moving mass. The simply supported pipe conveying fluid has a circular hollow cross-section. The crack is assumed to be always open during vibrations. The crack compliance is modeled by using the strain energy release rate relation.

2. Theory and formulations

The system with a moving mass on the cracked simply supported pipe conveying fluid is shown in Fig. 1, where m_m is a moving mass, v is the velocity of the moving mass, u is the velocity of fluid flow, L is the total length of the pipe, and x_c is the position of the crack from the left-hand support. Fig. 2 shows a circular hollow cross-section of the cracked section. θ_c and $2b$ are the crack depth(severity) and the length of a crack, respectively. Two equations of motion are derived for the two parts of the pipe located on the left and on the right of the cracked section. Fig. 3 represents the modeling of the cracked element. A local flexibility matrix connecting two undamaged pipe segments represents the crack section.

2.1. Energy of the pipe and moving mass

By using the assumed mode method, the transverse displacement $y(x, t)$ of a cracked simply supported pipe can be assumed to be as

$$y(x, t) = \sum_{n=1}^{\mu} \phi_n(x)q_n(t), \tag{1}$$

where $q_n(t)$ are generalized coordinates which is time dependent, μ is the total number of the generalized coordinates, and $\phi_n(x)$ are spatial mode functions of a simply supported beam missing the fluid and a moving

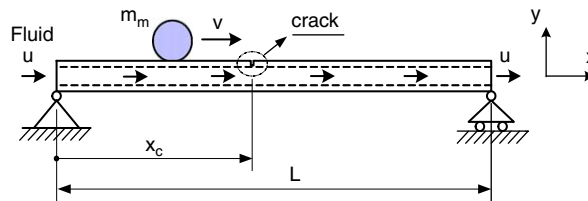


Fig. 1. Geometry of the cracked simply supported pipe with a moving mass.

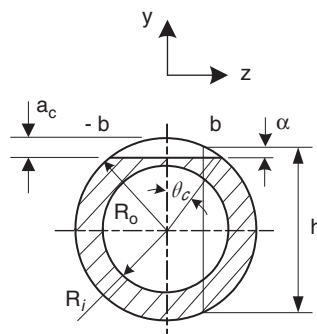


Fig. 2. Cross-section of the cracked pipe.

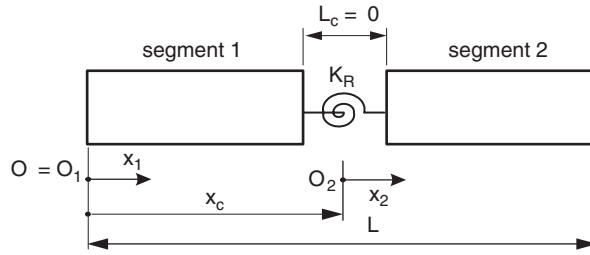


Fig. 3. Modeling of the cracked element.

mass. In Fig. 1 the energy of the cracked pipe can be written as

$$T_p = \frac{1}{2} \sum_{n=1}^{\mu} \sum_{k=1}^2 \left[m \int_0^{L_k} \phi_{nk}^2(x) dx \dot{q}_n^2(t) \right], \tag{2}$$

$$V_p = \frac{1}{2} \sum_{n=1}^{\mu} \sum_{k=1}^2 \left[EI \int_0^{L_k} \{\phi_{nk}''(x)q_n(t)\}^2 dx \right] + \frac{1}{2} K_R(\Delta y'_c)^2. \tag{3}$$

In Eq. (3), the quantity

$$\Delta y'_c = \left. \frac{dy}{dx} \right|_{x_2=0} - \left. \frac{dy}{dx} \right|_{x_1=x_c} \tag{4}$$

represents the jumps in the rotation. The kinetic energy of the moving mass can be expressed as [6]

$$T_m = \frac{1}{2} m_m \sum_{n=1}^{\mu} \sum_{k=1}^2 \{v^2 q_n^2(t) \phi_{nk}'^2(x_m) + 2v q_n(t) \dot{q}_n(t) \phi_{nk}(x_m) \phi_{nk}'(x_m) + \dot{q}_n^2(t) \phi_{nk}^2(x_m) + v^2\}, \tag{5}$$

where (\cdot) denotes the $\partial/\partial t$, and (\prime) represents the $\partial/\partial x$. In addition, m is mass per unit length of the pipe, K_R is bending stiffness, and EI means bending stiffness coefficient. k is the number of the segments (Fig. 3). Since the horizontal velocity of the moving mass is v , the horizontal displacement of the moving mass x_m is

$$x_m = f_m(t) = \int_0^t v dt \quad (0 \leq x_m \leq L). \tag{6}$$

2.2. Work and energy due to the fluid flow

The kinetic energy of the fluid flow inside the pipe can be expressed as [31]

$$T_f = \frac{1}{2} m_f \sum_{n=1}^{\mu} \sum_{k=1}^2 \left[\int_0^{L_k} \{u^2 + 2u \phi_{nk}(x_f) \dot{q}_n(t) \phi_{nk}(x_f) q_n(t) + \{\phi_{nk}(x_f) \dot{q}_n(t)\}^2\} dx_f \right] \quad (x_f = ut, 0 \leq x_f \leq L), \tag{7}$$

where m_f is the fluid mass per unit length of a pipe. The work of a follower force due to the fluid discharge is divided into two kinds of work, one is the work done by conservative force component, and the other is the work done by non-conservative force component. The work W_c due to the conservative component of a tangential follower force is

$$W_c = \frac{1}{2} \sum_{n=1}^{\mu} \sum_{k=1}^2 \int_0^{L_k} m_f u^2 \{\phi_{nk}'(x_f) q_n(t)\}^2 dx_f. \tag{8}$$

The work δW_{nc} due to the non-conservative component of a follower force is

$$\delta W_{nc} = - \sum_{n=1}^{\mu} m_f \{ \phi'_{n2}(L) \phi_{n2}(L) \} q_n(t) \delta q_n(t) = 0. \tag{9}$$

2.3. Boundary conditions

The boundary conditions of a cracked simply supported pipe are

$$\begin{aligned} \text{for } x = 0, \quad \phi_{n1}(0) = 0 \quad \text{and} \quad \frac{\partial^2 \phi_{n1}(0)}{\partial x^2} = 0, \\ \text{for } x = L, \quad \phi_{n2}(L) = 0 \quad \text{and} \quad \frac{\partial^2 \phi_{n2}(L)}{\partial x^2} = 0. \end{aligned} \tag{10}$$

The boundary conditions for the transverse deflection, bending moment, shear force and slope at the cracked section ($x = x_c$) are

$$\begin{aligned} \phi_{n1}(x_c) = \phi_{n2}(x_c), \quad \frac{\partial^2 \phi_{n1}(x_c)}{\partial x^2} = \frac{\partial^2 \phi_{n2}(x_c)}{\partial x^2}, \quad \frac{\partial^3 \phi_{n1}(x_c)}{\partial x^3} = \frac{\partial^3 \phi_{n2}(x_c)}{\partial x^3}, \\ \frac{\partial \phi_{n2}(x_c)}{\partial x} - \frac{\partial \phi_{n1}(x_c)}{\partial x} = \frac{EI}{K_R} \frac{\partial^2 \phi_{n2}(x_c)}{\partial x^2}. \end{aligned} \tag{11}$$

2.4. Crack modeling

Consider the bending vibrations of a uniform Euler–Bernoulli beam in the x – y plane, which is assumed to be a plane of symmetry for any cross-section. The crack is assumed to be always open. The additional strain energy due to the crack can be considered in the form of a flexibility coefficient expressed in terms of the stress intensity factor, which can be derived by Castigliano’s theorem in the linear elastic range. Therefore, the local flexibility in the presence of the width $2b$ of a crack is defined by [20]

$$C_{ij} = \frac{\partial u_{ij}}{\partial P_j} = \frac{\partial^2}{\partial P_i \partial P_j} \left(\int_{-b}^b \int_0^{a_c} J(\alpha) \, d\alpha \, dz \right), \tag{12}$$

where P_i is the load in the same direction as the displacement and $J(\alpha)$ is the strain energy density function. The function is

$$J(\alpha) = \frac{1}{E^*} (K_{IM})^2, \tag{13}$$

where $E^* = E/(1 - \nu_p^2)$ for the plane strain and ν_p is Poisson’s ratio. The stress intensity factor for the bending moment is given by

$$K_{IM} = \frac{M}{\pi R^2 t_p} \sqrt{\pi R \theta_c} F_b(\theta_c), \tag{14}$$

where $R = (R_o + R_i)/2$ is the mean radius. θ_c is the half-angle of the total through-wall crack (the crack severity will be indicated by θ_c/π as percentage [15]) and

$$F_b(\theta_c) = 1 + A_t \left[4.5967 \left(\frac{\theta_c}{\pi} \right)^{1.5} + 2.6422 \left(\frac{\theta_c}{\pi} \right)^{4.24} \right], \tag{15}$$

where

$$\begin{aligned} A_t &= \left(0.125 \frac{R}{t_p} - 0.25 \right)^{0.25} \quad \text{for } 5 \leq \frac{R}{t_p} \leq 10, \\ A_t &= \left(0.4 \frac{R}{t_p} - 3.0 \right)^{0.25} \quad \text{for } 10 \leq \frac{R}{t_p} \leq 20, \end{aligned} \tag{16}$$

where t_p is the thickness of the pipe. Substituting Eqs. (14)–(16) into Eq. (13), the flexible matrix due to the crack can be obtained.

2.5. Equation of motion

2.5.1. Dimensionless equation of motion

The equation of motion of the system is obtained by substituting the above work and energy functions into the Lagrange’s equation.

$$\frac{d}{dt} \left(\frac{\partial L_a}{\partial \dot{q}_i} \right) - \left(\frac{\partial L_a}{\partial q_i} \right) = 0, \tag{17}$$

where L_a can be defined as follows:

$$L_a \equiv (T_p + T_m + T_f - V_p) + W_c + \delta W_{nc}. \tag{18}$$

For simplicity, the following dimensionless parameters are introduced:

$$\begin{aligned} \xi &= \frac{x}{L}, \quad \xi_f = \frac{x_f}{L} = uL \sqrt{\frac{m}{EI}} \tau, \quad \tau = \frac{t}{L^2} \sqrt{\frac{EI}{m}}, \\ M_m &= \frac{m_m}{mL}, \quad U = uL \sqrt{\frac{m_f}{EI}}, \quad L_k^* = \frac{L_k}{L}, \quad \xi_c = \frac{x_c}{L}, \\ \beta &= \frac{m_m L}{\sqrt{mEI}} \bar{v}, \quad \gamma = \frac{m_m L^3}{EI} \bar{v}^2, \quad d = \frac{q}{L}, \quad M_f = \frac{m_f}{m}, \\ \xi_m &= \frac{x_m}{L} = \bar{v} L^2 \sqrt{\frac{m}{EI}} \tau, \quad K_R^* = \frac{K_R L}{EI}, \end{aligned} \tag{19}$$

where \bar{v} is v/L . Therefore, the dimensionless equation of motion is obtained in matrix form as follows:

$$\mathbf{M} \ddot{\mathbf{d}} + \mathbf{C} \dot{\mathbf{d}} + \mathbf{K} \mathbf{d} = \mathbf{0}, \tag{20}$$

where (\cdot) denotes the $\partial/\partial\tau$ and (\prime) stands for the $\partial/\partial\xi$. The matrices of Eq. (20) can be written respectively as

$$\mathbf{M} = \sum_{n=1}^{\mu} \sum_{k=1}^2 \left\{ \int_0^{L_k^*} \phi_{nk}^2(\xi) d\xi + M_f \int_0^{L_k^*} \phi_{nk}^2(\xi_f) d\xi_f + M_m \phi_{nk}^2(\xi_m) \right\}, \tag{21a}$$

$$\mathbf{C} = \sum_{n=1}^{\mu} \sum_{k=1}^2 \left\{ M_f \int_0^{L_k^*} \frac{d}{d\tau} \{ \phi_{nk}^2(\xi_f) \} d\xi_f + M_m \frac{d}{d\tau} \{ \phi_{nk}^2(\xi_m) \} \right\}, \tag{21b}$$

$$\begin{aligned} \mathbf{K} &= \sum_{n=1}^{\mu} \sum_{k=1}^2 \left[\int_0^{L_k^*} \{ \phi_{nk}''(\xi) \}^2 d\xi + \beta \left\{ \frac{d}{d\tau} \{ \phi_{nk}'(\xi_m) \} \phi_{nk}(\xi_m) + \frac{d}{d\tau} \{ \phi_{nk}(\xi_m) \} \phi_{nk}'(\xi_m) \right\} \right. \\ &\quad - \gamma \{ \phi_{nk}'(\xi_m) \}^2 + \sqrt{M_f} U \int_0^{L_k^*} \left\{ \frac{d}{d\tau} \{ \phi_{nk}'(\xi_f) \} \phi_{nk}(\xi_f) + \frac{d}{d\tau} \{ \phi_{nk}(\xi_f) \} \phi_{nk}'(\xi_f) \right\} d\xi_f \\ &\quad \left. - U^2 \int_0^{L_k^*} \{ \phi_{nk}'(\xi_f) \}^2 d\xi_f + K_R^* \{ \phi_{n2}'(\xi_2 = 0) - \phi_{n1}'(\xi_1 = \xi_c) \}^2 \right]. \end{aligned} \tag{21c}$$

2.5.2. Modal formulation

Eq. (20) can be transformed into the following equation:

$$\mathbf{M}^* \dot{\boldsymbol{\eta}} + \mathbf{K}^* \boldsymbol{\eta} = \mathbf{0}. \tag{22}$$

For the complex modal analysis, it is assumed that $\boldsymbol{\eta}$ is a harmonic function of τ expressed as

$$\boldsymbol{\eta} = e^{\lambda\tau} \boldsymbol{\Theta}, \tag{23}$$

where λ is the eigenvalue, and Θ is the corresponding mode shape. From the eigenvalues in Eqs. (22), (23), the frequencies can be obtained.

3. Numerical results and discussion

In this study, the dynamic behavior of the cracked simply supported pipe influenced by the moving mass, the crack severity ratio $\theta^* (= \theta/\pi)$, and the position ratio of the crack $\xi_c (= x_c/L)$ are computed by the fourth-order Runge–Kutta method. To illustrate this response, the pipe of the length 1 m, out-radius $R_o = 0.1$ m, and in-radius $R_i = 0.08$ m was considered (Young’s modulus = 210 GPa, mass density = 7860 kg/m³).

We have studied the dimensionless mid-span deflection of the simply supported pipe for the first mode of vibration, and the frequency variations of the cracked simply supported pipe for the first two modes of vibration. The frequency ratio is defined as

$$\Omega = \frac{\omega(\text{cracked frequency})}{\omega_0(\text{un-cracked frequency})} \tag{24}$$

Figs. 4–7 represent the dimensionless mid-span deflection for a cracked pipe conveying fluid with a moving mass due to the crack, a moving mass and fluid, respectively. In figures, the horizontal axis is the position of the moving mass, and the axis of the ordinates are the dimensionless mid-span deflection ($d/|d_{\max}|$) of the cracked pipe.

Fig. 4 shows the dimensionless mid-span deflection for a cracked pipe conveying fluid with $M_m = 0.3$, $U = 0.1$, and $\xi_c = 0.3$. The velocity of moving mass is 1 m/s. When the moving mass velocity and the fluid velocity are constant, the mid-span deflection of the simply supported pipe is proportion to the crack severity ratio. As the crack severity ratio is increased, the position of the moving mass that makes the maximum mid-span deflection of the simply supported pipe is moved to the rear bound of the pipe. In $\theta^* = 0.05$, the maximum mid-span deflection of the pipe occurs at $\xi = 0.62$, a distance from the left-hand support. In $\theta^* = 0.15$, the maximum mid-span deflection of the pipe occurs at $\xi = 0.75$.

Fig. 5 represents the dimensionless mid-span deflection of a cracked pipe conveying fluid according to the crack position ratios for $v = 1$ m/s, $U = 0.1$, and $\theta^* = 0.1$. These results mean that when the crack is located at the center its effect is the largest on the mid-span deflection of the cracked simply supported pipe conveying fluid. Comparing Fig. 4 with Fig. 5, the mid-span deflection of the cracked pipe conveying fluid is more sensitive to the crack severity ratio than to the position ratio of the crack.

Fig. 6 shows the variation of the mid-span deflection of the cracked pipe conveying fluid with the moving mass for the four velocities of the fluid. When the velocity of the moving mass is constant, the dimensionless mid-span deflection of the simply supported pipe is proportional to the velocity of the fluid. The difference of maximum mid-span deflection of the cracked pipe in the two case of $U = 0.5$ and 1.5 is about 11.21%.

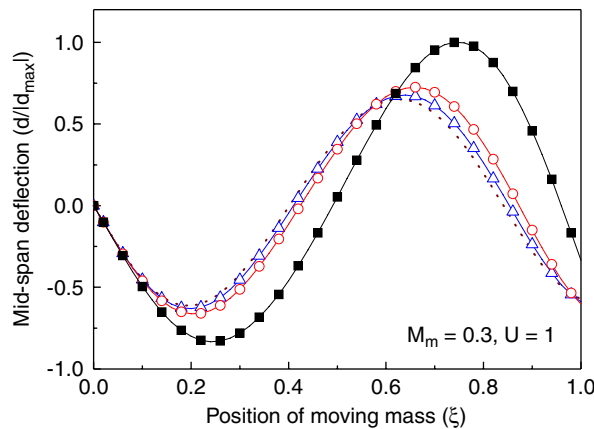


Fig. 4. Mid-span deflections of the cracked pipe for: $M_m = 0.3$, $U = 1.0$, $v = 1$ m/s, $\xi_c = 0.3$, $\theta^* = 0.05$; —▲—, $\theta^* = 0.10$; —○—, $\theta^* = 0.15$; —■—, $\theta^* = 0.20$.

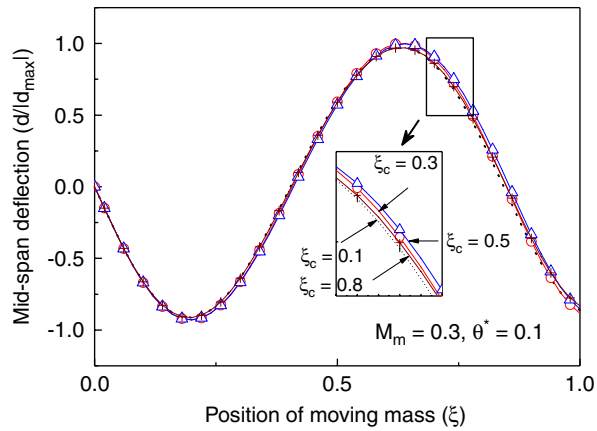


Fig. 5. Mid-span deflections of the cracked pipe for: $M_m = 0.3, \theta^* = 0.1, v = 1 \text{ m/s}, U = 1.0$. \dots , $\xi_c = 0.1$; $\text{---}\circ\text{---}$, $\xi_c = 0.3$; $\text{---}\triangle\text{---}$, $\xi_c = 0.5$; $\text{---}\blacksquare\text{---}$, $\xi_c = 0.8$.

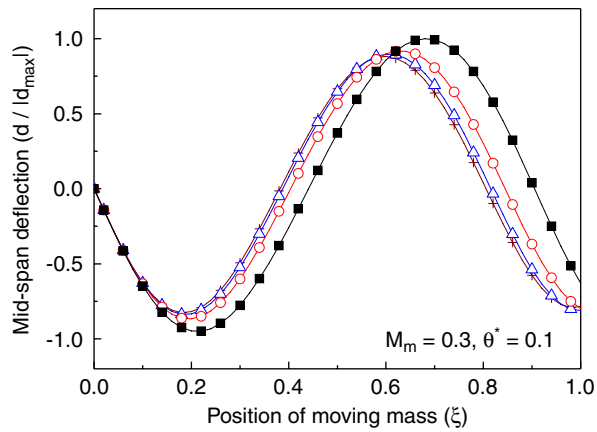


Fig. 6. Mid-span deflections of the cracked pipe for: $M_m = 0.3, \theta^* = 0.1, v = 1 \text{ m/s}, \xi_c = 0.3$. $\text{---}\circ\text{---}$, $U = 0.0$; $\text{---}\triangle\text{---}$, $U = 0.5$; $\text{---}\circ\text{---}$, $U = 1.0$; $\text{---}\blacksquare\text{---}$, $U = 1.5$.

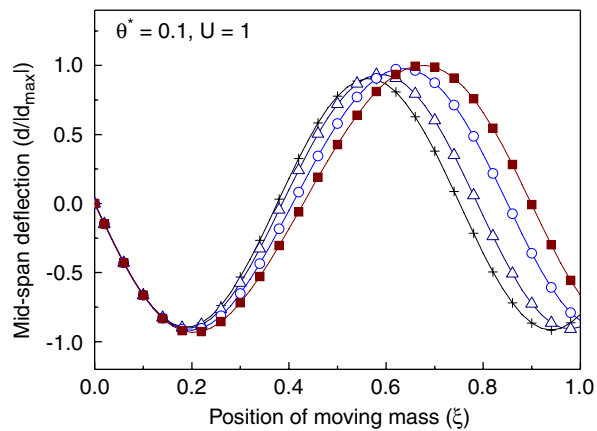


Fig. 7. Mid-span deflections of the cracked pipe for: $U = 1.0, \theta^* = 0.1, v = 1 \text{ m/s}, \xi_c = 0.3$. $\text{---}\times\text{---}$, $M_m = 0$; $\text{---}\triangle\text{---}$, $M_m = 0.1$; $\text{---}\circ\text{---}$, $M_m = 0.3$; $\text{---}\blacksquare\text{---}$, $M_m = 0.5$.

The variation of mid-span deflection of a cracked pipe conveying fluid according to the moving mass is shown in Fig. 7. In curves the crack severity ratio, the position ratio of the crack and the velocity of the moving mass are 0.1, 0.3 and 1 m/s, respectively. Totally, as the moving mass is increased, the mid-span deflection of the simply supported pipe conveying fluid is increased. As the moving mass is increased, the position of the moving mass that appears the maximum mid-span deflection of the simply supported pipe is gradually moved to the rear bound of the pipe. These are the results by the coupling between the moving mass and the velocity of the moving mass.

Figs. 8 and 9 present the frequency ratios of a cracked pipe for the first two modes for the variations of the crack severity ratio and the position ratio of the crack with $M_m = 0.3$ and $U = 0.1$, respectively. The horizontal axis is the position of the moving mass, the axis of the ordinates are the frequency ratios of the cracked simply supported pipe conveying fluid with the moving mass. In Fig. 8, the frequency ratios of the simply supported pipe are in inverse proportion to the crack severity ratio in the first mode of vibration. Fig. 8(b) shows the frequency ratios of a cracked pipe for the second mode of vibration. In Fig. 9(a), when the crack position exists in the center of the simply supported pipe conveying fluid, the frequency ratio has the smallest value. In Fig. 9(b), when the crack position exists in the center of the simply supported pipe conveying fluid, its frequency ratio is always unit for every position of the moving mass. That is, this system has the same frequency as the un-cracked pipe. This is the reason that the crack located at the node of the second mode of vibration. In Fig. 9, every curve shows that the lowest value of frequency ratio appears when the moving mass moves up on the crack position.

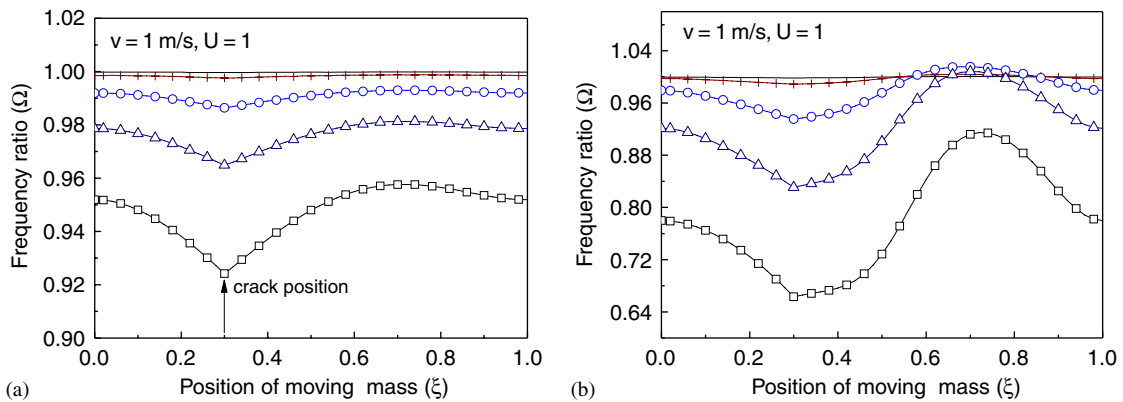


Fig. 8. Frequency ratios of the cracked pipe for: $U = 1.0$, $M_m = 0.1$, $v = 1 \text{ m/s}$, $\xi_c = 0.3$. (a) First mode; (b) second mode. —, $\theta^* = 0.05$; —+, $\theta^* = 0.08$; —o, $\theta^* = 0.12$; —\Delta, $\theta^* = 0.15$; —\square, $\theta^* = 0.18$.

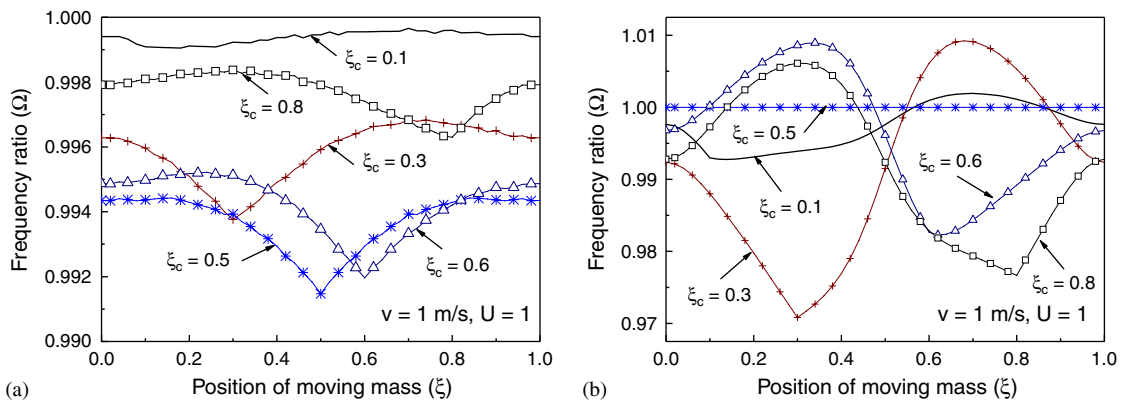


Fig. 9. Frequency ratios of the cracked pipe for: $U = 1.0$, $M_m = 0.3$, $v = 1 \text{ m/s}$, $\theta^* = 0.1$. (a) First mode; (b) second mode. —, $\xi_c = 0.1$; —+, $\xi_c = 0.3$; *—, $\xi_c = 0.5$; —\Delta, $\xi_c = 0.6$; —\square, $\xi_c = 0.8$.

Figs. 10 and 11 present the frequency of a cracked pipe conveying fluid with the moving mass according to the variation of the fluid velocity and the moving mass, respectively. In these figures, the unit of frequency is $1/(\text{dimensionless time}; \tau)$. The crack severity ratio θ^* is 0.1, the position ratio of the crack ξ_c is 0.3, and the velocity of moving mass is 1 m/s. Totally, the frequencies of the simply supported pipe are in inverse proportion to the velocity of fluid in the each modes of vibration. When the position of the moving mass exists in the center of the simply supported pipe conveying fluid, the difference of frequencies of the cracked pipe in the two case of $U = 0.5$ and 1.5 is about 11.3% for the first mode of vibration. In Fig. 11(a), as the moving mass is increased, the frequency of the simply supported pipe conveying fluid is decreased. When the position of the moving mass exists in the center of the simply supported pipe conveying fluid, the difference of frequencies of the cracked pipe in the two case of $M_m = 0$ (natural frequency) and $M_m = 0.1$ is about 7.21%. And the difference of frequencies of the cracked pipe in the two case of $M_m = 0.1$ and 0.3 is about 13.6%.

Fig. 12 shows the natural frequency reduction of the first and second modes of vibration. As shown in the figure, the reduction in natural frequency is related to the severity ratio and the position ratio of the crack, and the mode shapes. In this case, it is without the moving mass.

The frequency ratios due to the crack parameters (crack position and crack severity), the fluid velocity and the moving mass are presented in Table 1. In Table 1, the frequency ratios of the second mode of vibration are unit. When the crack position ratio is 0.8, the frequency ratio of the cracked pipe with $U = 1$ and $M_m = 0.3$ has the larger value than the frequency ratio of the un-cracked pipe. The result is the influence of moving mass.

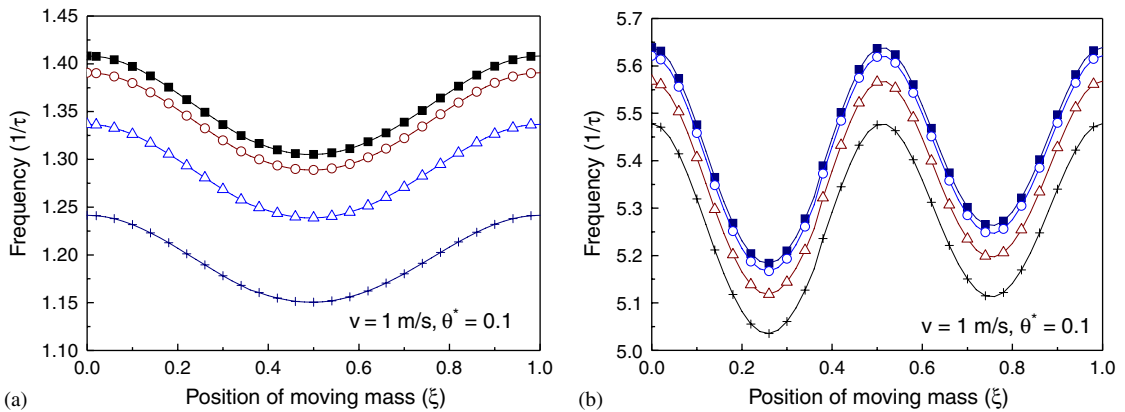


Fig. 10. Frequency variations of the cracked pipe for: $M_m = 0.3$, $\theta^* = 0.1$, $v = 1$ m/s, $\xi_c = 0.3$. (a) First mode. \blacksquare , $U = 0$; \circ , $U = 0.5$; \blacktriangle , $U = 1.0$; \times , $U = 1.5$; (b) second mode. \blacksquare , $U = 0$; \circ , $U = 0.5$; \blacktriangle , $U = 1.0$; \times , $U = 1.5$.

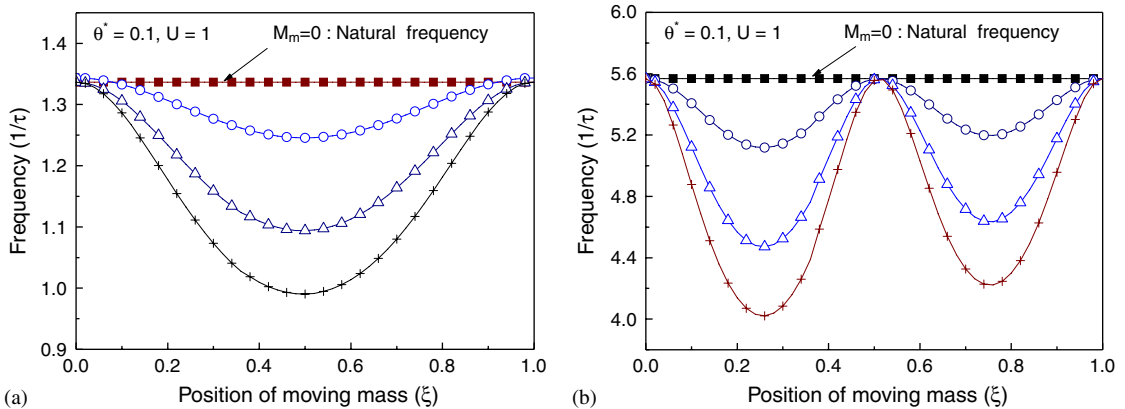


Fig. 11. Frequency variations of the cracked pipe for: $U = 1.0$, $\theta^* = 0.1$, $v = 1$ m/s, $\xi_c = 0.3$. (a) First mode. \blacksquare , $M_m = 0$; \circ , $M_m = 0.1$; \blacktriangle , $M_m = 0.3$; \times , $M_m = 0.5$; (b) second mode. \blacksquare , $M_m = 0$; \circ , $M_m = 0.1$; \blacktriangle , $M_m = 0.3$; \times , $M_m = 0.5$.

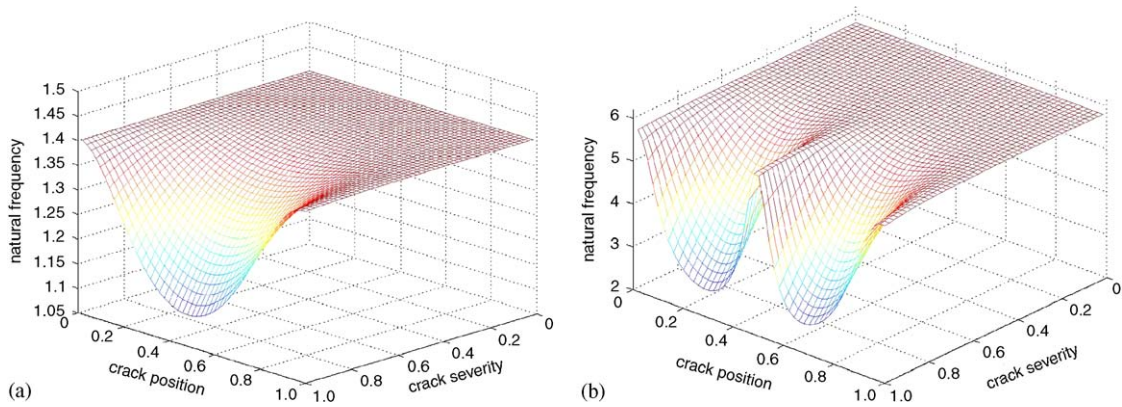


Fig. 12. Variations of natural frequencies with crack position and crack severity: (a) first mode, (b) second mode.

Table 1

Frequency ratios for crack parameters (crack position and crack severity), fluid velocity, and moving mass ($v = 1 \text{ m/s}$)

Crack position (ξ_c)	Crack severity (θ^*)	Natural frequency ($U = 0, M_m = 0$)		Natural frequency ($U = 1.0, M_m = 0$)		Frequency ($U = 1.0, M_m = 0.3$)	
		First mode	Second mode	First mode	Second mode	First mode ($\xi = 0.5$) ^a	Second mode ($\xi = 0.25$)
		0.3	0.08	0.9983	0.9973	0.9985	0.9974
	0.12	0.9903	0.9788	0.9919	0.9793	0.9910	0.9452
	0.15	0.9745	0.9201	0.9786	0.9213	0.9764	0.8536
0.5	0.08	0.9974	1.000	0.9978	1.000	0.9966	1.000
	0.12	0.9852	1.000	0.9877	1.000	0.9816	1.000
	0.15	0.9616	1.000	0.9675	1.000	0.9529	1.000
0.8	0.08	0.9999	0.9998	0.9992	0.9974	0.9992	1.002
	0.12	0.9946	0.9813	0.9955	0.9819	0.9955	1.009
	0.15	0.9857	0.9361	0.9881	0.9374	0.9879	1.004

^a ξ (position of the moving mass from the left-hand support, x/L).

Fig. 13 makes a comparison between our results and Mahmoud’s results [7] on the studies of the cracked and un-cracked beam without fluid flow, where the velocity of a moving mass is 50 m/s and the length of the beam is 50 m. These show that our curves are in good agreement with the Mahmoud’s curves for the mid-span deflection of the cracked and un-cracked beam. Fig. 14 shows the damping effect of the fluid flow on the mid-span deflection of the un-cracked pipe with a moving mass, where the velocity of a moving mass is 20 m/s, the length of the pipe is 10 m, and the velocity of the fluid flow is 10 m/s. The deflection of the pipe unconsidering the damping effect of the fluid flow [32] is about 9.46% larger than our results. So the damping effect of the fluid flow is one of the factors that must be considered on the studies of the dynamic behavior of the pipe.

4. Conclusions

In this paper, the influences of the crack severity and moving mass have been studied on the dynamic behavior of the cracked simply supported pipe conveying fluid by the numerical method. The cracked pipe has been treated as two undamaged segments connected by a rotational elastic spring at the cracked section. The

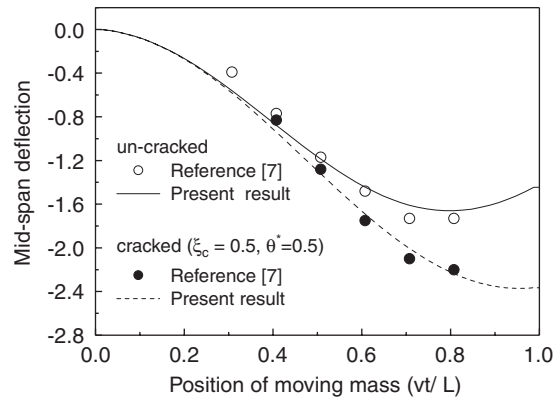


Fig. 13. Mid-span deflection of cracked and un-cracked beam.

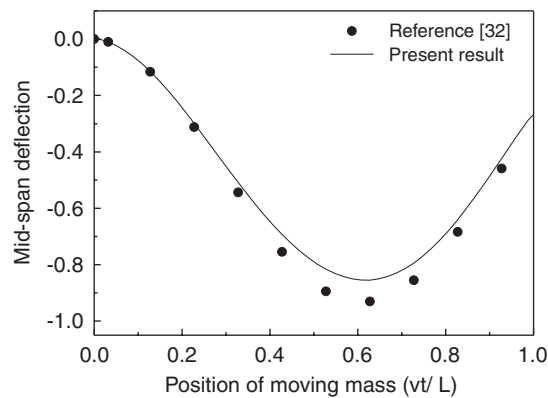


Fig. 14. Mid-span deflection of cracked pipe.

stiffness of the spring depends on the crack severity and the geometry of the cracked section. The main conclusions are the following.

(1) When the moving mass and the velocity of fluid are constant, the mid-span deflection of the cracked simply supported pipe is proportional to the crack severity ratio.

(2) The mid-span deflection of the cracked pipe conveying fluid is more sensitive to the crack severity ratio than to the crack position ratio.

(3) As the moving mass and the fluid velocity are increased, the mid-span deflection of the cracked simply supported pipe conveying fluid is increased.

(4) When the crack position exists in center of the pipe conveying fluid, its frequency ratio has the smallest value for the first mode of vibration. At this position of the crack, the frequency ratio is always unit and independent of the crack severity ratio for the second mode of vibration.

(5) The frequencies of cracked simply supported pipe conveying fluid are in inverse proportion to the fluid velocity and the moving mass, respectively.

These study results will contribute to the safety test and stability estimation of structures of a cracked pipe conveying fluid with a moving mass.

References

- [1] T.B. Benjamin, Dynamics of a system of articulated pipes conveying fluid (I. Theory), *Proceedings of the Royal Society (London), Series A* 261 (1961) 457–468.

- [2] Y. Sugiyama, K. Katayama, E. Kanki, K. Nishino, B. Åkesson, Stabilization of cantilevered flexible structures by means of an internal flowing fluid, *Journal of Fluids and Structures* 10 (1996) 653–661.
- [3] H.P. Lee, The dynamic response of a Timoshenko beam subjected to a moving mass, *Journal of Sound and Vibration* 198 (2) (1996) 249–256.
- [4] M.M. Staniscic, On a new theory of the dynamic behavior of the structures carrying moving masses, *Ingenieur-Archiv* 55 (1985) 176–185.
- [5] H.P. Lee, Dynamic response of a beam with a moving mass, *Journal of Sound and Vibration* 191 (2) (1995) 289–294.
- [6] H.I. Yoon, J.T. Jin, I.S. Son, A study on dynamic behavior of simply supported fluid flow pipe with crack and moving mass, *Proceedings of the 11th International Congress on Sound and Vibration*, 2004, pp. 2215–2222.
- [7] M.A. Mahmoud, C.S. Abou Zaid, Dynamic response of a beam with a crack subject to a moving mass, *Journal of Sound and Vibration* 256 (4) (2002) 591–603.
- [8] T.G. Chondros, A.D. Dimarogonas, Identification of crack in welded joints of complex structures, *Journal of Sound and Vibration* 69 (1980) 531–538.
- [9] T.G. Chondros, A.D. Dimarogonas, Dynamic sensitivity of structures to cracks, *Journal of Vibration and Acoustics, Stress and Reliability in Design* 111 (1989) 251–256.
- [10] T.G. Chondros, A.D. Dimarogonas, Vibration of a cracked cantilever beam, *Journal of Vibration and Acoustics, Transactions of the American Society of Mechanical Engineers* 120 (1998) 742–746.
- [11] W.M. Ostachowicz, M. Krawczuk, Analysis of the effect of cracks on the natural frequencies of a cantilever beam, *Journal of Sound and Vibration* 150 (1991) 191–201.
- [12] C. Zhu, D.A. Robb, D.J. Ewins, The dynamics of a cracked rotor with an active magnetic bearing, *Journal of Sound and Vibration* 265 (2003) 469–487.
- [13] S. Christides, A.D.S. Barr, One-dimensional theory of cracked Bernoulli–Euler beams, *International Journal of Mechanical Sciences* 26 (11/12) (1984) 639–648.
- [14] M.H.F. Dado, O. Abuzeid, Coupled transverse and axial vibratory behaviour of cracked beam with end mass and rotary inertia, *Journal of Sound and Vibration* 261 (2003) 675–696.
- [15] D. Liu, H. Gurgenci, M. Veidt, Crack detection in hollow section structures through coupled response measurements, *Journal of Sound and Vibration* 261 (2003) 17–29.
- [16] S.C. Fan, D.Y. Zheng, Stability of a cracked Timoshenko beam column by modified Fourier series, *Journal of Sound and Vibration* 264 (2003) 475–484.
- [17] D.Y. Zheng, S.C. Fan, Vibration and stability of cracked hollow-sectional beams, *Journal of Sound and Vibration* 267 (2003) 933–954.
- [18] S.M. Murigendrappa, S.K. Maiti, H.R. Srirangrajan, Experimental and theoretical study on crack detection in pipes filled with fluid, *Journal of Sound and Vibration* 270 (2004) 1013–1032.
- [19] J. Wauer, On the dynamics of cracked rotors: a literature survey, *Applied Mechanics Review* 43 (1) (1990) 13–17.
- [20] A.D. Dimarogonas, Vibration of cracked structures: a state of the art review, *Engineering Fracture Mechanics* 55 (5) (1996) 831–857.
- [21] G. Bammios, A. Trochides, Dynamic behavior of a cracked cantilever beam, *Applied Acoustics* 45 (1995) 97–112.
- [22] T.G. Chondros, A.D. Dimarogonas, Vibration of a cracked cantilever beam, *Transactions of the ASME* 120 (1998) 742–746.
- [23] E.I. Shifrin, R. Ruotolo, Natural frequencies of a beam with an arbitrary number of cracks, *Journal of Sound and Vibration* 222 (3) (1999) 409–423.
- [24] S.M. Cheng, X.J. Wu, W. Wallace, A.S.J. Swamidas, Vibrational response of a beam with a breathing crack, *Journal of Sound and Vibration* 225 (1) (1999) 201–208.
- [25] J.H. Kuang, B.W. Huang, The effect of blade crack on mode localization in rotating bladed disks, *Journal of Sound and Vibration* 227 (1) (1999) 85–103.
- [26] I. Takahashi, Vibration and stability of non-uniform cracked Timoshenko beam subjected to follower force, *Computers and Structures* 71 (1999) 585–591.
- [27] L. Nobile, Mixed crack initiation and direction in beams with edge crack, *Theoretical and Applied Fracture Mechanics* 33 (2000) 107–116.
- [28] M. Kisa, J. Brandon, The effect of closure of cracks on the dynamics of a cracked cantilever beam, *Journal of Sound and Vibration* 238 (1) (2000) 1–18.
- [29] E. Viola, L. Federici, L. Nobile, Detection of crack location using cracked beam element method for structural analysis, *Theoretical and Applied Fracture Mechanics* 36 (2001) 23–35.
- [30] Y. Bammios, E. Douka, A. Trochidis, Crack identification in beam structures using mechanical impedance, *Journal of Sound and Vibration* 256 (2) (2002) 287–297.
- [31] H.I. Yoon, I.S. Son, Dynamic behavior of cracked pipe conveying fluid with moving mass based on Timoshenko beam theory, *KSME International Journal* 18 (12) (2004) 2216–2224.
- [32] H.I. Yoon, S.H. Lim, J.S. Yu, Influence of two moving masses on dynamic behavior of a simply supported pipe conveying fluid flow, *Proceedings of the Eighth International Congress on Sound and Vibration*, Hong Kong, China, 2001, pp. 2835–2842.